photonics

MDPI

Article

Polycationic Photosensitizers as Effective Anticancer Agents That Destroy Cancer Stem Cells, Cancer Vascularization and Induce Protective Desmoplastic Reaction around Lung Cancers

Evgeniya Kogan [1], Gennady Meerovich [2,3], Saida Karshieva [4,5], Elena Makarova [6], Igor Romanishkin [2,*], Ekaterina Akhlyustina [3], Irina Meerovich [7], Nikolay Zharkov [8], Sergey Kharnas [9], Vladimir Levkin [9,*], Sofya Demura [1], Zhilong Chen [10], Victor Loschenov [2,3] and Igor Reshetov [11]

[1] Institute of Clinical Morphology and Digital Pathology, I.M. Sechenov First Moscow State Medical University (Sechenov University), Moscow 119992, Russia; kogan_e_a@staff.sechenov.ru (E.K.); demura_s_a@staff.sechenov.ru (S.D.)
[2] Prokhorov General Physics Institute of the Russian Academy of Sciences, Moscow 119991, Russia; meerovich@nsc.gpi.ru (G.M.); loschenov@nsc.gpi.ru (V.L.)
[3] Institute of Engineering Physics for Biomedicine, National Research Nuclear University MEPhI, Moscow 115409, Russia; evakhlyustina@mephi.ru
[4] N.N. Blokhin National Medical Research Center of Oncology, Moscow 115478, Russia; karshieva.ss@misis.ru
[5] Research and Educational Center of Biomedical Engineering, National University of Science and Technology MISIS, Moscow 119049, Russia
[6] Organic Intermediates and Dyes Institute, Moscow 123001, Russia; eamakarova@niopik.ru
[7] A.N. Bach Institute of Biochemistry, Research Center of Biotechnology of the Russian Academy of Sciences, Moscow 119071, Russia; imeerovich@inbi.ras.ru
[8] Center of Digital Biodesign and Personalized Healthcare, I.M. Sechenov First Moscow State Medical University (Sechenov University), Moscow 119992, Russia; zharkov_n_v@staff.sechenov.ru
[9] N.V. Sklifosovskiy Institute of Clinical Medicine, I.M. Sechenov First Moscow State Medical University (Sechenov University), Moscow 119992, Russia; kharnas_s_s@staff.sechenov.ru
[10] Huadong Hospital, Fudan University, Shanghai 200433, China; chenzhilong@fudan.edu.cn
[11] L.L. Levshin Institute of Cluster Oncology, I.M. Sechenov First Moscow State Medical University (Sechenov University), Moscow 119992, Russia; reshetov_i_v@staff.sechenov.ru
* Correspondence: igor.romanishkin@nsc.gpi.ru (I.R.); levkin_v_v@staff.sechenov.ru (V.L.)

Abstract: PDT using PSs based on polycationic derivatives of synthetic bacteriochlorin against Lewis lung carcinoma provides effective inhibition of tumor growth with an increase in the lifespan and survival of mice in the group. PDT with polycationic photosensitizers destroys CSCs and tumor neovascularization, and activates the desmoplastic reaction. These results open up new opportunities for increasing the effectiveness of treatment and reducing the incidence of relapses and metastases after PDT.

Keywords: photodynamic therapy; photosensitizer; polycationic bacteriochlorin; cancer stem cells; Lewis lung carcinoma; vascularization; desmoplastic reaction

Citation: Kogan, E.; Meerovich, G.; Karshieva, S.; Makarova, E.; Romanishkin, I.; Akhlyustina, E.; Meerovich, I.; Zharkov, N.; Kharnas, S.; Levkin, V.; et al. Polycationic Photosensitizers as Effective Anticancer Agents That Destroy Cancer Stem Cells, Cancer Vascularization and Induce Protective Desmoplastic Reaction around Lung Cancers. *Photonics* **2024**, *11*, 485. https://doi.org/10.3390/photonics11060485

Received: 16 January 2024
Revised: 8 April 2024
Accepted: 17 May 2024
Published: 21 May 2024

1. Introduction

Early diagnosis, overcoming resistance to traditional methods of therapy of highly lethal malignant tumors, is one of the most important tasks of modern medicine. Among the malignant human cancers, lung cancer is the most common and one of the most fatal. It accounts for approximately 30% of deaths from all types of malignant neoplasms among the male population. In addition, in the vast majority (75%) of cases, it is diagnosed at late stages, when surgical treatment is no longer possible [1–4]. Even after surgery and comprehensive neoadjuvant, target, and multimodal therapies (including photodynamic therapy, PDT), survival rates for patients diagnosed with bronchogenic carcinoma remain extremely low. Therefore, the development of new approaches to therapy is necessary. The most promising of these approaches are methods that can kill cancer stem cells and their

habitat—their niches. The aggressive behavior of lung cancer and its metastasis are based on the presence of cancer stem cells (CSCs) [5]. Lung cancer CSCs are verified according to their markers (CD44, CD133, CD34, Oct4) [6–8].

CSCs contribute to the limited effectiveness of therapeutic approaches for treating oncological diseases. Cancer cells form a hierarchy within a tumor based on their degree of maturity, and ability to proliferate and differentiate. CSCs are the ancestors of this hierarchy, localized in special niches containing vessels and mesenchymal components. They are in a dormant state, resistant to apoptosis, rarely divide, and produce progeny of proliferated cancer cells while maintaining the cancer clone. CSCs participate in invasive growth, metastasis, and cancer relapses due to epithelial–mesenchymal transformation [9,10]. CSCs are resistant to chemotherapy and radiation therapy due to their ability to resist apoptosis and to remain dormant with autophagy, and their having special antitoxic genes and their products (ALDH1 and others) [10]. It has been shown that CSCs are sensitive to certain photodynamic effects [11–17].

To optimize the photosensitizer (PS) and treatment regimen and improve antitumor treatment results, it is necessary to study the therapeutic pathomorphosis of tumor tissue after PDT, in addition to macro-criteria. The main criteria for tumor pathomorphosis after the photodynamic treatment are: the proportion of damaged cancer cells with necrosis, the survival of tumor cells, the degree of apoptosis of tumor tissue cells (by the key enzyme Caspase-3), the number of mitotic figures and the their average proportion in the treated tumor area, the mitotic index by the proliferation marker Ki-67, as well as the damage to CSCs and the neovascularization feeding the tumor, and severity of desmoplastic reaction (DR) of normal tissues at the border of the tumor.

Necrosis is the most common type of cell death in living tissue. It occurs with the activation of lysosomal enzymes of the cell itself, leading to the breakdown of its damaged components. A demarcation inflammatory reaction develops at the boundaries of living and dead tissue with phagocytosis of necrotic masses and subsequent replacement of its connective tissue. Necrosis markers cause the lysis of cell nuclei and cytoplasm, karyopyknosis, karyorrhexis, and cytoplasmic coagulation [3].

In contrast, apoptosis is a programmed form of cell death that involves the activation of endonucleases and cutting of DNA molecules in the nucleosome region. The cell turns on the "suicide" program when damage is severe, resulting in apoptosis. The apoptotic enzyme Caspase-3 is a hub molecule that binds various apoptotic factors and is a key marker for detecting apoptotic process [3].

The preservation of cell viability is mainly indicated by mitosis and the number of proliferating cells, as determined by the mitotic index. The expression of the nuclear protein Ki-67 is closely related to the proliferation and growth of tumor cells and is widely used as a marker of proliferation.

Vascularization is a necessary biological condition for malignant tumor growth, which is ensured by the tumor itself through two processes: neoangiogenesis and vasculogenesis. Neoangiogenesis is the formation of new vessels from pre-existing capillaries of adjacent normal tissue. Vasculogenesis takes place in embryonic tissue and involves the transformation of stem cells into vascular endothelium. It can be assumed that vasculogenesis can also occur in malignant tumors, but with the participation of CSCs. Some mechanisms of photodynamic inhibition of cancer growth are associated with the suppression of blood supply to the cancerous node [18].

Desmoplastic reaction (DR) is the growth of fibrous connective tissue and infiltration of the mesenchymal cells origin (lymphocytes, macrophages, myofibroblasts, endothelium) resulting in the formation of a fibrous capsule around a benign scar after tumor treatment. DR is an important local reaction of antiblastic defense [3].

Effective inhibition of CSCs is only achieved with sufficiently high levels of photodynamic exposure [13,15]. The area of aggressive tumor growth and invasion into the adjacent normal tissue is mainly located in the depth of tissue. Therefore, light must pass through the entire thickness of the cancerous node from the illuminated surface of the lung

to reach this area. To ensure a high level of photodynamic exposure in this area, necessary for CSC destruction, it is important to use PSs with high absorbance in the near infrared range (700–800 nm). This spectral range has minimal intrinsic absorption by the cancerous tissue, and is also known as the "spectral window of biological tissue transparency" [19].

Previously, a tetracationic derivative of synthetic bacteriochlorin with high extinction in the spectral region of about 760 nm was synthesized in work [20]. It demonstrated acceptable pharmacokinetics and accumulation selectivity, and high dose-dependent photodynamic efficiency in vitro against human A549 and mice LLC lung cancer cells, as well as in vivo against LLC lung cancer. We have improved the composition of these compounds and the technology for their preparation, which made it possible to create polycationic new bacteriochlorin derivatives. Based on a comparison of the results of photodynamic exposure of A549 lung carcinoma cells with these polycationic derivatives of bacteriochlorin and anionic aluminum sulfophthalocyanine [13], it was suggested that cancer cells may be more sensitive to cationic PSs compared to anionic ones. It has also been suggested that polycationic derivatives of synthetic bacteriochlorin are more effective against CSCs [17], although quantitative data were obtained in different cell cultures [14].

In a previous in vivo study [21], we demonstrated macro-criteria of PDT efficacy on LLC with these PSs, which induced a high level of tumor necrosis and apoptosis, and a sharp decrease in proliferative activity of cancer cells, including CSCs. Therefore, PSs based on new polycationic derivatives of synthetic bacteriochlorins are promising for PDT of cancers. The objective of this work is to study and analyze the pathomorphosis of LLC after PDT with these PSs, including their effectiveness against CSCs and tumor neovascularization, as well as their ability to induce a high level of desmoplastic reaction, which is an important aspect of anti-blastoma protection of healthy tissue and blocking tumor invasion.

2. Materials and Methods

2.1. Photosensitizers

Aqueous solutions of tetracationic (3-PyBrE)$_4$BCBr$_4$ and octacationic (3-PyEPy)$_4$BCBr$_8$ were used as PSs [22]. In vitro studies of these compounds against A549 human lung cancer cells showed their high phototoxicity (IC_{50} = 0.69 μM and 0.57 μM) and low cytotoxicity (IC_{50} > 200 μM) [17].

2.2. Tumor Model

The research involving animals was conducted in accordance with the international recommendations outlined in the "European Convention for the Protection of Vertebrate Animals used for Experimental and other Scientific Purposes" (Strasbourg, France, 1987).

The LLC cells were cultured in RPMI 1640 medium containing 2 mM glutamine, an antimycotic-antibiotic solution (100 U penicillin, 100 μg streptomycin, and 250 ng amphotericin B per mL), and 10% fetal calf serum at 37 °C and 5% CO_2. Upon reaching 80% confluence, the cells were detached with 0.25% trypsin-EDTA solution, washed, counted, and resuspended in 100 μL of phosphate-buffered saline. The LLC cells were inoculated intramuscularly into the right leg of BALB/c mice at a rate of 100,000 cells per mouse. Inoculation of tumors was carried out simultaneously for all mice.

2.3. Photodynamic Studies

In accordance with [23], the mice were split into 3 major groups: two groups for PDT with (3-PyBrE)$_4$BCBr$_4$ and (3-PyEPy)$_4$BCBr$_8$ (n = 21 each), a control group with intact tumors (n = 21). For partial control groups (group with irradiation but no PS, n = 8, and two groups with PS but no irradiation, n = 8 each), there were no significant differences from intact. As such, the data from partial control groups are not presented here. The PS solutions were administered via tail vein injection in a dose of 8 mg/kg on day 5 after the inoculation with the LLC carcinoma, when the average volume of the tumor node was 0.12 ± 0.1 cm^3 in all groups. Irradiation began 180 min after intravenous administration.

The tumor node was irradiated with 765 nm light from an LED light source with a light power density of 120 mW/cm^2, measured using a PM160T power meter (Thorlabs, Newton, NJ, USA), and a dose density of 260 J/cm^2. The macro-criteria for the antitumor efficacy of the studied PSs against LLC carcinoma (the tumor growth inhibition, TGI, the average life span of animals in the control and the irradiated groups, ALS_c and ALS_i, respectively, and life span increase, LSI) were evaluated in [21].

2.4. Morphological Analysis

Cancer and adjacent tissues were studied on serial 4 μm thick paraffin sections with prefixation of tissues in 10% neutral formalin according to standard technique [2] in control and experimental groups.

Histology was analyzed on sections stained with hematoxylin and eosin. It was possible to evaluate cancer, its borderline with adjacent normal tissue, with invasion, and desmoplastic reaction in the border. In cancer, we compare the square of necrotic foci in 10 fields of view at 600×. Mitotic activity per 3000 tumor cells and the vessels in the tumor tissue were counted in 10 fields of view at 600×, and the percentage of mitotic figures.

The tumor invasiveness into the intact muscle tissue was assessed microscopically (in expert points, semi-quantitatively): absence of invasion—0 points, low invasion—2 points, moderate—4 points, prominent—6 points). In cancer tissue we estimated area of necrosis in 10 fields of view at 600×, mitotic figures in cancer tissue per 3000 tumor cells, and the tumor vessels in the tumor in 10 fields of view at 600×.

The severity of the desmoplastic reaction was also assessed microscopically (in expert points, semi-quantitatively). A very poor desmoplastic reaction at the border of the tumor and normal tissue (0–2 points) was characterized by individual macrophages, lymphoid elements, and myofibroblasts. The moderate desmoplastic reaction (4 points) was characterized by a wave of macrophages, lymphoid elements and myofibroblasts, fibroblasts, and single eosinophils. A prominent desmoplastic reaction (6 points) was characterized with a predominance of myofibroblastic and fibroblastic reactions. An intense desmoplastic reaction (8 points) is characterized by the appearance of newly formed vessels in combination with macrophages, lymphoid elements, myofibroblasts, fibroblasts, and granulation tissue.

2.5. Immunohistochemistry (IHC)

The proliferation index of tumor cells was assessed immunohistochemically by the proliferation marker Ki-67, the degree of apoptosis in the tumor tissue by the key apoptosis enzyme Caspase-3, and the viability of CSCs by the expression of stemness markers ALDH1, CD34, and CD133 on serial 4 μm thick paraffin sections. Immunohistochemical markers were studied by monoclonal and polyclonal antibodies (Rabbit polyclonal antibody, Huabio, Hangzhou HuaAn Biotechnology Co. Ltd., Hangzhou, China), Ki-67 (Rabbit monoclonal antibody, GeneTex, Irvine, CA, USA), Oct4, and CD44 (Recombinant rabbit monoclonal antibody, Huabio Hangzhou HuaAn Biotechnology Co. Ltd., China). Secondary antibody kit (Conjugated Goat anti-Rabbit IgG Ultra Polymer, Huabio Hangzhou HuaAn Biotechnology Co. Ltd., Hangzhou, China, RTU), and DAB kit (DAB Substrate Kit, Cell Marque, Rocklin, CA, USA) were used.

IHC was carried out according to the standard method using antigen unmasking in a microwave oven [24]. Positive and negative controls were used for IHC reactions. As negative controls, samples of the studied sections were taken, which were subjected to a standard IHC procedure, but without the addition of primary antibodies. Positive controls for each antibody were selected according to the manufacturer's specifications. The results of IHC reactions were evaluated as a percentage of positively stained cells per 3000 cells.

Images were acquired using a light microscope (Olympus BX45, Shinjuku City, Tokyo, Japan) fitted with a digital camera.

2.6. Statistical Analysis of Morphological Data

The obtained results were compared between each group at different times of the experiment. Statistical analysis was performed using a non-parametric Wilcoxon *t*-test [25].

3. Results

3.1. Macro-Criteria of Antitumor Efficacy of Photosensitizers

Evaluation of TGI after PDT with $(3\text{-PyBrE})_4BCBr_4$ and $(3\text{-PyEPy})_4BCBr_8$ at administered dose of 8 mg/kg and calculation of TGI compared to the control group were performed for 21 days after irradiation. The proportion of the surviving mice after PDT and LSI were calculated at 90 days after the experiment. The obtained results demonstrate high antitumor efficacy of the studied PSs (Table 1).

Table 1. Macro-criteria of antitumor efficacy of photosensitizers $(3\text{-PyBrE})_4BCBr_4$ and $(3\text{-PyEPy})_4BCBr_8$ after PDT with the administered dose of 8 mg/kg and light dose density 260 J/cm^2.

Group	TGI_{max}, %	ALS, Days	LSI, %	Surviving Mice, %
Control	—	28.3 ± 6	—	0
$(3\text{-PyBrE})_4BCBr_4$	80	56.0 ± 18.7	97	16.7
$(3\text{-PyEPy})_4BCBr_8$	85	67.2 ± 20.8	137	50

3.2. Evaluation of the Antitumor Efficacy of PSs Based on the Results of Morphological and Immunohistochemical Studies of Tumor Tissues

Histological examination of LLC cells after the PDT with $(3\text{-PyBrE})_4BCBr_4$ and $(3\text{-PyEPy})_4BCBr_8$ shows an increased rate of necrosis and apoptosis (Figure 1, Table 2). Necrosis of cancer is characterized by nuclear lysis and cytoplasm coagulation. Apoptotic cells are shrunken, karyopyknotic, with formation of apoptotic bodies. Lymphomacrophage infiltration and desmoplastic reaction (myofibroblastic and fibroblastic cells) can be seen in the border between tumor and adjacent normal tissue. We have found the decrease in the invasiveness of the cancerous tissue and activation of desmoplastic borderline reaction in the group treated with $(3\text{-PyEPy})_4BCBr_8$ compared to the $(3\text{-PyBrE})_4BCBr_4$ group after PDT compared to the control (Table 3).

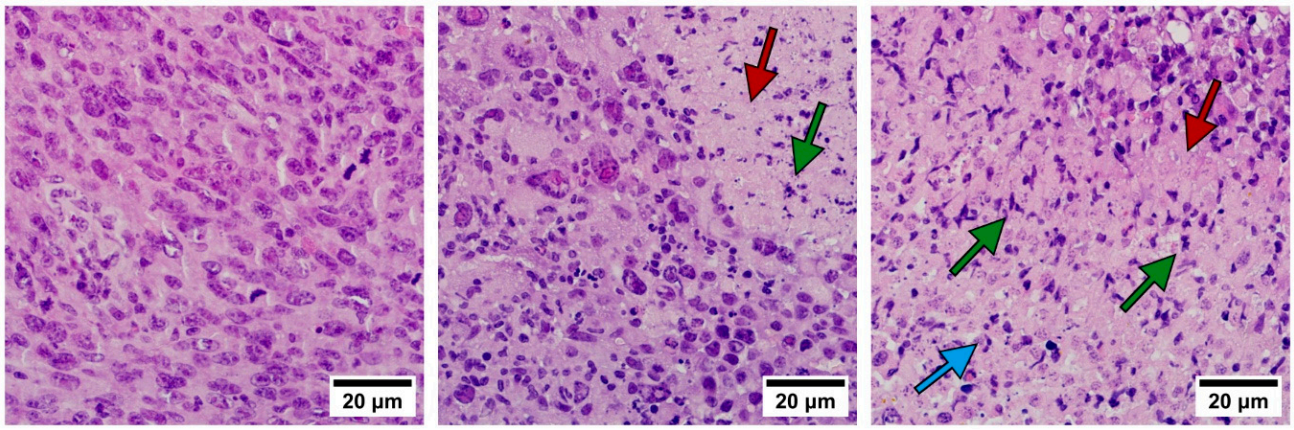

Figure 1. Control (intact tumors) and tumors after PDT with $(3\text{-PyBrE})_4BCBr_4$ and $(3\text{-PyEPy})_4BCBr_8$ on day 14 of the experiment. Necrosis—red arrow, apoptosis—green arrow, desmoplastic reaction with granulation tissue—blue arrow. Hematoxylin and eosin.

Table 2. Percentages of necrosis, surviving cancer tissue, and mitosis among intact cancer cells in control and in PDT-treated groups on day 14 after irradiation.

Group	Necrosis, %	Surviving Cancer Tissue, %	Mitosis, %
Control	25.0	75.0	13.4 ± 1.3
$(3\text{-PyBrE})_4BCBr_4$	69.0	31.0	2.4 ± 0.2
$(3\text{-PyEPy})_4BCBr_8$	97.5	2.5	0.3 ± 0.2

Table 3. Tumor invasiveness and desmoplastic reaction (in points) at the "cancer–preserved muscle tissue" border in control and in PDT-treated groups on day 14 after irradiation.

Group	Cancer Invasiveness, Points	Desmoplastic Reaction, Points
Control	6.0	2.0
$(3\text{-PyBrE})_4BCBr_4$	2.0	6.0
$(3\text{-PyEPy})_4BCBr_8$	0.0	8.0

3.3. The Immunohistochemical Examination of the Pathomorphosis of LLC

LLC in control is characterized by high expression of Ki-67 (up to 84.9%), and a low level of apoptosis in intact cancer tissue (up to 4.8% cells by the expression of Caspase-3) (Figure 2).

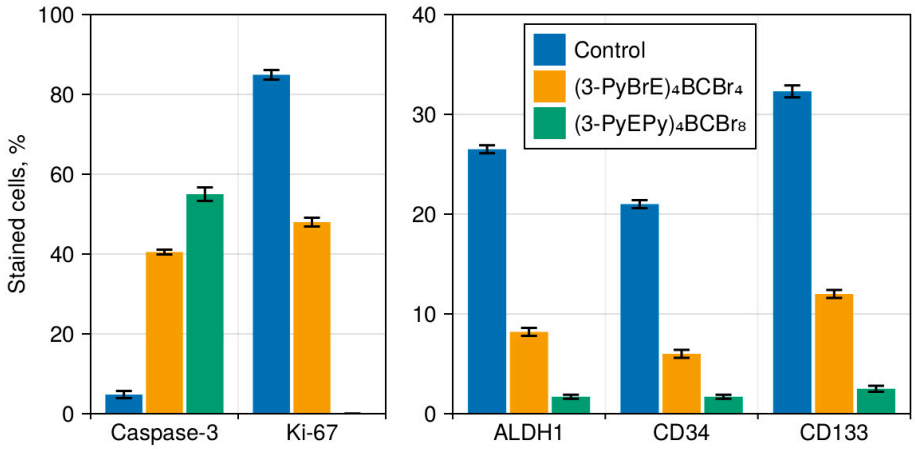

Figure 2. Immunohistochemical criteria for the efficacy of PDT with $(3\text{-PyBrE})_4BCBr_4$ and $(3\text{-PyEPy})_4BCBr_8$. Data from partial control not shown.

The immunohistochemical study of the groups after PDT revealed a significant decrease in the proliferative activity of the tumor (according to the values of the proliferation marker Ki-67), which decreases to 48% after PDT with $(3\text{-PyBrE})_4BCBr_4$ and to 0% for $(3\text{-PyEPy})_4BCBr_8$ (proliferating tumor cells after PDT with this PS are not detected). Apoptosis detected by Caspase-3 increases to 40% and 55%, respectively, compared to the control group (Figure 2). The specificity of Ki-67 the expression in LLC cancer cells consisted in the clumped nature of the distribution of the reaction product in the nuclei of cancer cells. Caspase-3 was detected in apoptotic bodies and nuclei of dying cancer cells and CSCs as deposits of a brown product.

3.4. Cancer Stem Cells in LLC

Tumors contain a certain number of CSCs expressing ALDH1, CD34, and CD133 (Figure 2). According to the investigated markers, this percentage ranges from 20 to 30% of all cancer cells in the central and peripheral regions of tumors. The difference in the number of ALDH1+, CD34+, and CD133+ CSCs may be connected with their immunophenotype

heterogeneity that has been described for hepatomas [26]. ALDH1, CD34, and CD133 were detected in the cytoplasm of individual and small groups of 3–4 cancer cells. CD34 was detected in cancer cells forming tumor vessels (Figure 3). Partial control groups (not shown) exhibited similar expression characteristics to the control group. The number of ALDH1+, CD34+, and CD133+ CSCs in LLC decreased to 10% after PDT with $(3\text{-PyBrE})_4BCBr_4$ and to 1–2% after PDT with $(3\text{-PyEPy})_4BCBr_8$, and was accompanied by a decrease in their size and shrinkage of the cytoplasm, which is the sign of their apoptotic changes (Figure 4).

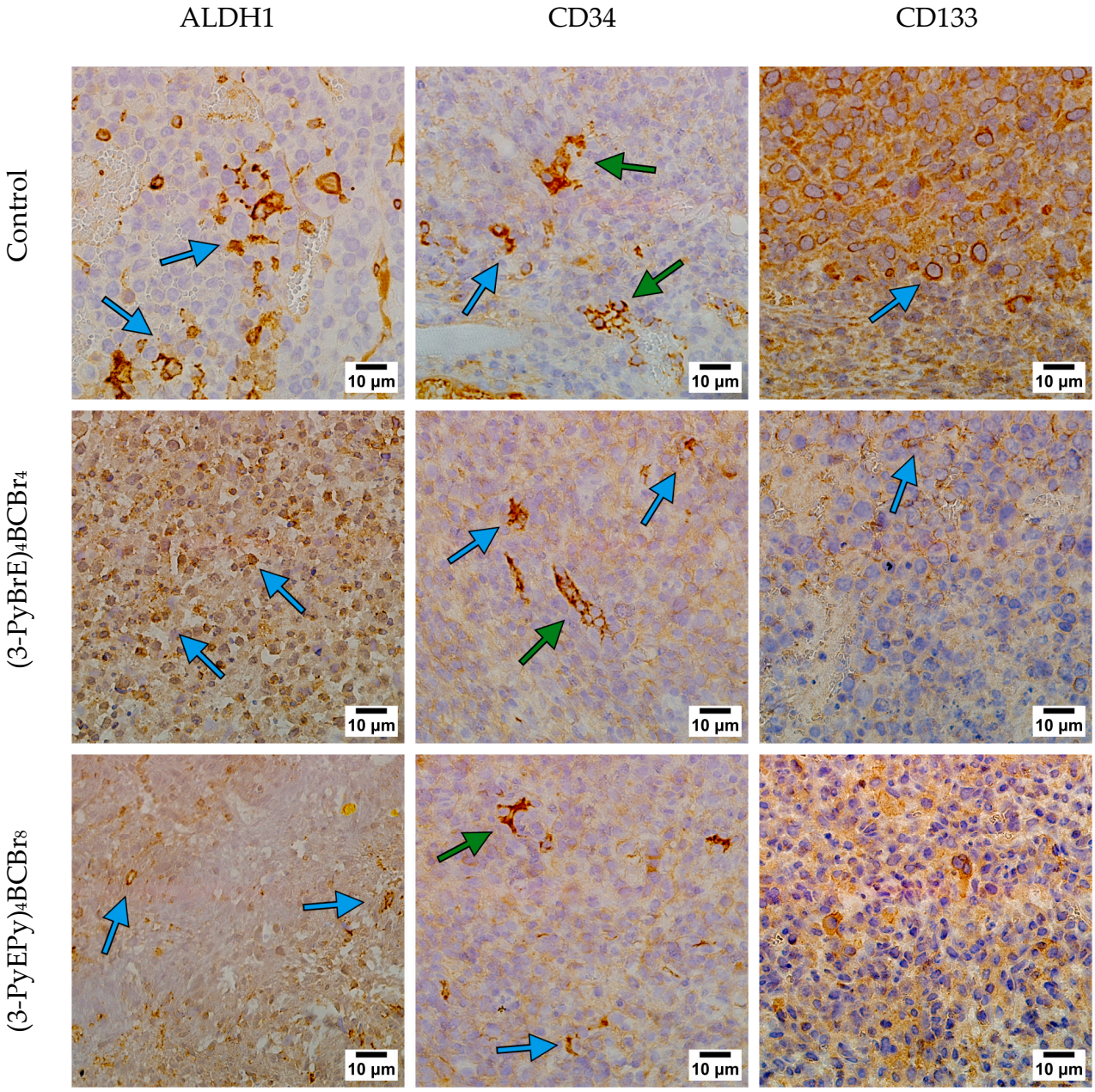

Figure 3. ALDH1, CD34 (CSCs—blue arrow, capillary the vessels of cancer—green arrow), CD133 in control (intact tumors) and in tumors after PDT with $(3\text{-PyBrE})_4BCBr_4$ and $(3\text{-PyEPy})_4BCBr_8$) on day 14 of experiment. Markers of CSCs—brown stained cytoplasm. Immunoperoxidase reaction with DAB.

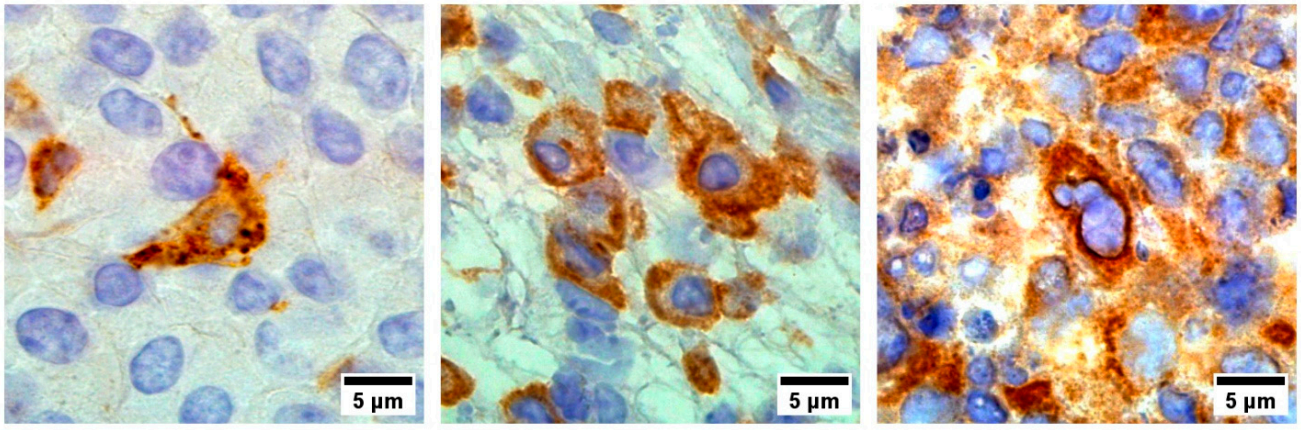

ALDH1 CD34 CD133

Figure 4. IHC markers of CSCs (×1000). Expression of the ALDH1, CD34, and CD133 stemness markers (brown cytoplasmic staining) in the LLC of control group.

Thus, according to immunohistochemical studies, PDT with $(3\text{-PyBrE})_4BCBr_4$ and $(3\text{-PyEPy})_4BCBr_8$ causes the death of a significant number of ALDH1+, CD34+, and CD133+ CSCs, stimulates apoptosis in CSCs and tumor tissue in general, and suppresses the proliferative activity of cancer cells and their mitotic activity. Moreover, all indicators induced by PDT with $(3\text{-PyEPy})_4BCBr_8$ are significantly more pronounced compared to $(3\text{-PyBrE})_4BCBr_4$ ($p < 0.05$).

3.5. Vascularisation in Tumor Tissue

In our study, to identify newly formed capillary-type vessels in tumors, we used CD34 antibodies, which are capable of detecting both the endothelium of newly formed vessels as well as CSCs. We have observed that CD34+ cancer stem cells participate in the formation of tumor vessels both in the tumors of the experimental and control groups (Figure 5).

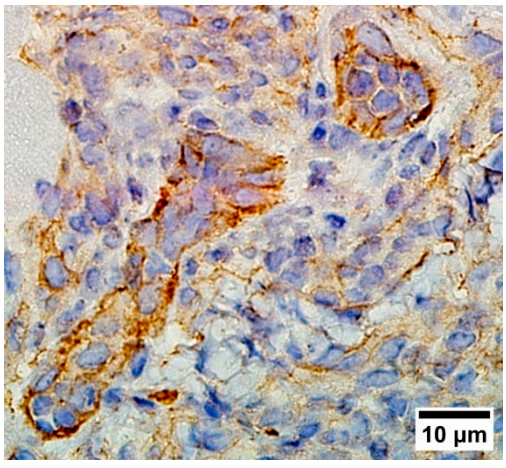

Figure 5. CD34+ cancer stem cells (brown stained cytoplasm) form tumor vessels in LLC (control). Erythrocytes visible in the lumen.

PDT with $(3\text{-PyBrE})_4BCBr_4$ and $(3\text{-PyEPy})_4BCBr_8$ after 7 and 14 days induced a decrease in the number of newly formed tumor vessels compared to the control group (Table 4, Figure 6), simultaneously with the number of CSCs, which proves the possible origin of tumor vessels from CSCs. A more pronounced inhibition of vascularization occurs in tumor tissue under the influence of $(3\text{-PyEPy})_4BCBr_8$. At the same time, hemorrhages and

vascular thrombosis are not observed in the treated tumor, and the vessels in the adjacent preserved muscle tissue remain intact as well as in the zone of DR (Figure 7).

Table 4. Vascularization in cancer tissue (mean density of capillary-type vessels in 10 fields of view at 400×).

Group	Interval after Irradiation, Days		
	3	**7**	**14**
Control	17	20	18
$(3\text{-PyBrE})_4BCBr_4$	7	5	3
$(3\text{-PyEPy})_4BCBr_8$	3	2	0

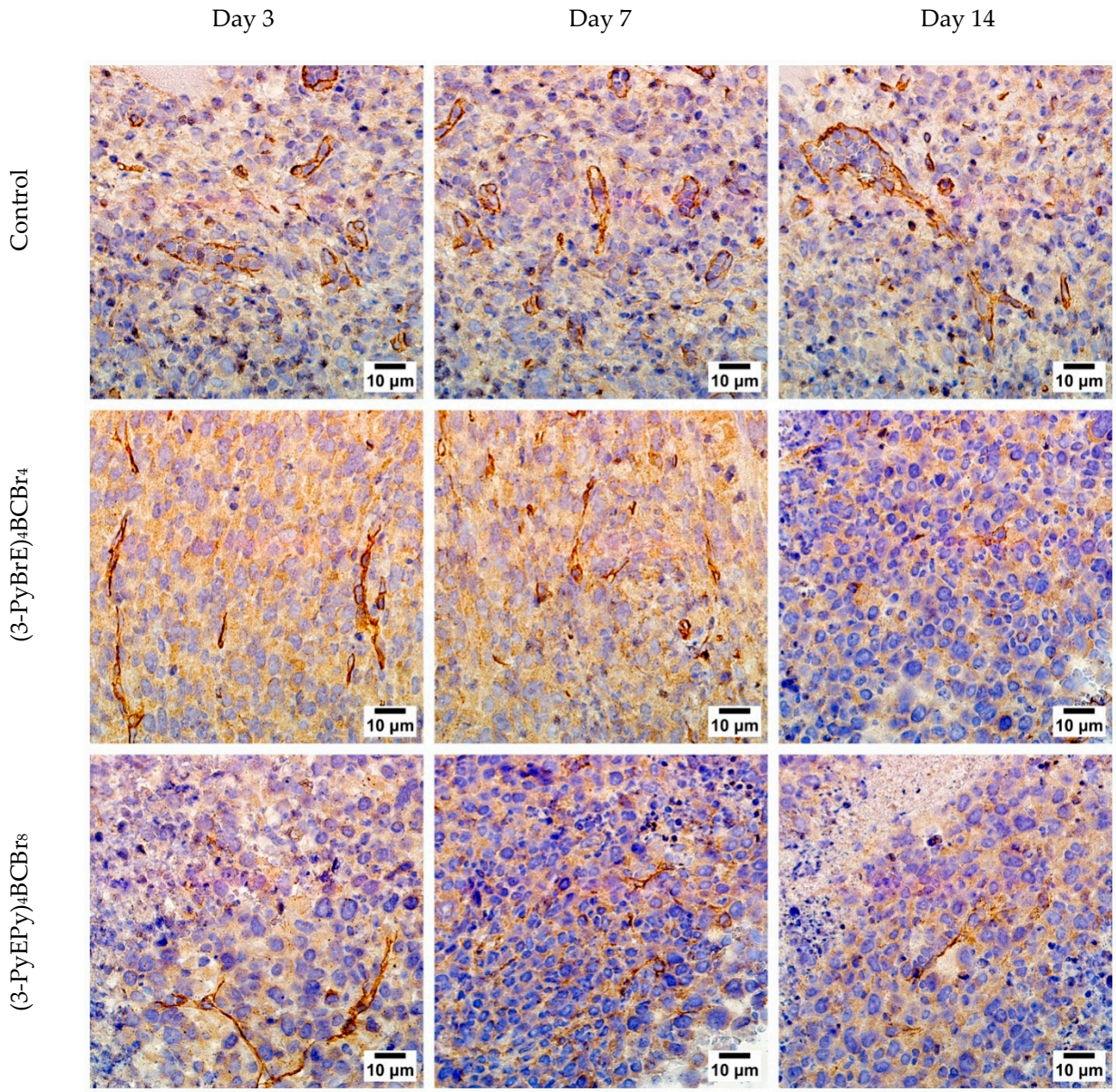

Figure 6. Vascularization of tumors (by expression of CD34 in the endothelium of tumor vessels, red arrow) in control (intact tumors) and tumors after PDT with $(3\text{-PyBrE})_4BCBr_4$ and $(3\text{-PyEPy})_4BCBr_8$ on days 3, 7, and 14 of the experiment. In the group after PDT with $(3\text{-PyEPy})_4BCBr_8$, single vessels with CD34+ endothelium on day 14 after irradiation. Immunoperoxidase reaction with DAB. Data from partial control not shown.

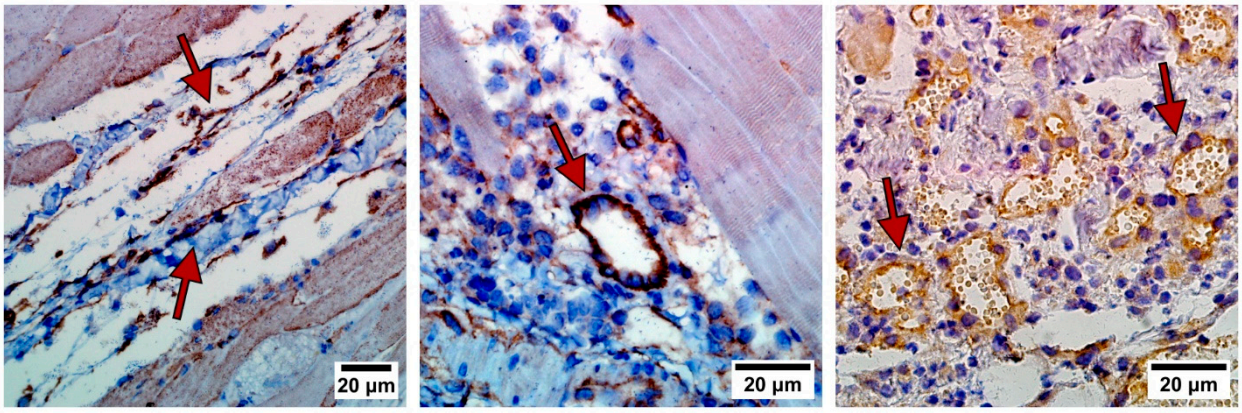

(**a**) (**b**) (**c**)

Figure 7. Expression of CD34 in the vascular endothelium (brown staining of the cytoplasm, red arrow) of: (**a**)—intact muscle tissue; (**b**,**c**)—in tissue of desmoplastic reaction at the border of lung cancer after PDT on the 14th day after irradiation. Immunoperoxidase reaction with DAB.

3.6. Desmoplastic Reaction in the Border of Cancer

DR is formed by normal cells of mesenchymal origin (macrophages, lymphoid elements and myofibroblasts, fibroblasts, endothelium) which have different structure, lack of cell atypia, and are 2–4 sizes smaller than cancer cells. Comparison of DR in control and PDT-treated groups showed significant differences (Table 3, Figure 8). DR in the control group was practically absent at the border between the tumor and the normal tissue, and was represented by individual macrophages, lymphoid elements and myofibroblasts during all 14 days of the experiment. In the group after PDT with $(3\text{-PyBrE})_4BCBr_4$, the moderate desmoplastic reaction (4 points) appears already on day 3 of the experiment and is characterized by a wave of macrophages, lymphoid elements and myofibroblasts, fibroblasts and single eosinophils. Then, it is intensified by days 7 and 14 of the experiment (6 points), when myofibroblastic reactions and fibroblastic elements begin to predominate. In the group after PDT with $(3\text{-PyEPy})_4BCBr_8$, a pronounced DR also appears on day 3 of the experiment (6 points) and is represented by a shaft of myofibroblasts, fibroblasts, macrophages, lymphoid elements, and individual eosinophils, which then intensifies by days 7 and 14 of the experiment (8 points), when the most prominent newly formed vessels appear and, in combination with macrophages, lymphoid elements, myofibroblasts, and fibroblasts, granulation tissue is forming a pseudocapsule around the tumor. The DR induced by PDT with $(3\text{-PyEPy})_4BCBr_8$ was more pronounced compared to $(3\text{-PyBrE})_4BCBr_4$.

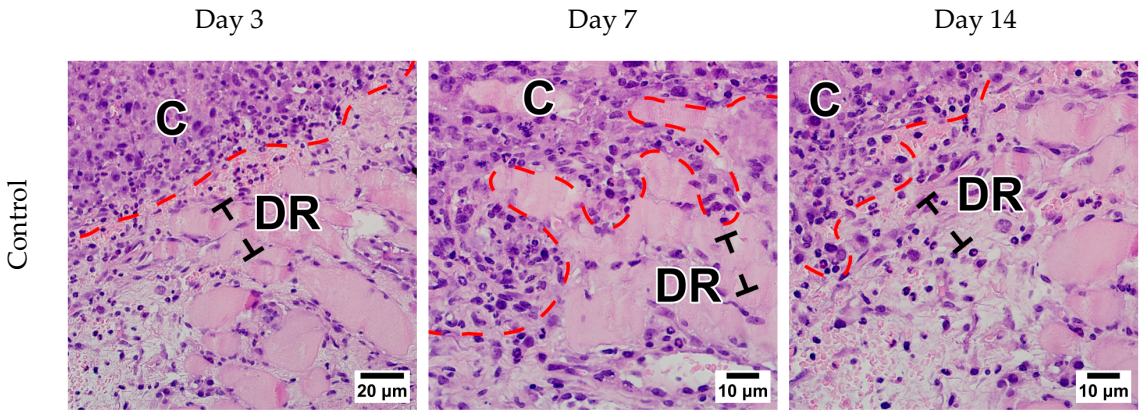

Figure 8. *Cont.*

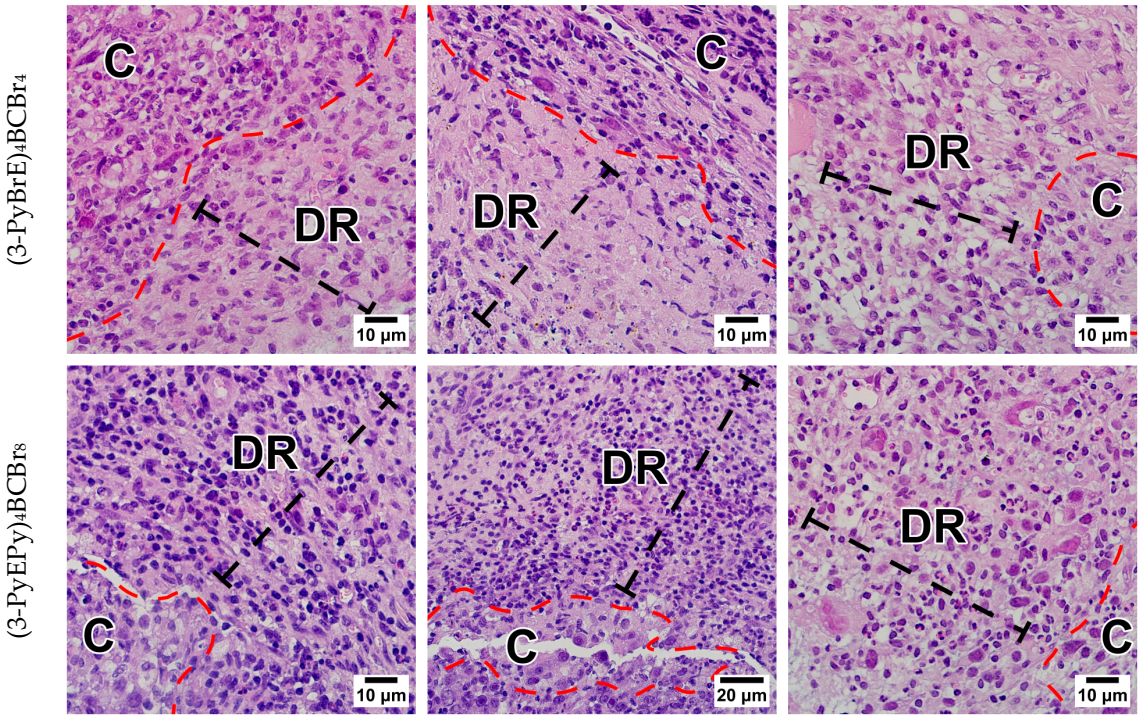

Figure 8. Increased severity of desmoplastic reaction in tumors after PDT with $(3\text{-PyBrE})_4BCBr_4$ and $(3\text{-PyEPy})_4BCBr_8$ on days 3, 7, and 14 of experiment compared with control (intact tumors). Border of cancerous tissue—red dashed line, area of desmoplastic reaction—DR. Histology, hematoxylin and eosin.

4. Discussion

In planning our experiments, we chose irradiation conditions taking into consideration methodological recommendations [23], work by other groups [13,14], and our previous experience. Photosensitizers based on bacteriochlorin derivatives have an advantage over the commonly used chlorin- or phthalocyanine-based PSs—their absorption maximum is shifted into a spectral range, minimally absorbed by the biological tissue, the "spectral window of biological tissue transparency" [19] (absorption maxima of the studied PSs were at 763 nm for $(3\text{-PyBrE})_4BCBr_4$ and 759 nm for $(3\text{-PyEPy})_4BCBr_8$, respectively). This absorption of the PS excitation light by the tissue can result in an undesired heating of the tissue, up to hyperthermia. The lowered tissue absorption also leads to higher efficiency of PS excitation, with a lower power density required to achieve a similar photodynamic effect. While tissue temperature was not controlled in this study, our previous studies showed that the tissue surface temperature increase does not exceed 2 °C at these power and dose densities.

PDT with polycationic derivatives of synthetic bacteriochlorin inhibits the growth of LLC in a mouse model and provides high antitumor effect, with tumor growth inhibition more than 85%, lifespan increase up to 137%, and overall survival in the group of 50%. The reasons for this are the death of cancer cells by necrosis and apoptosis and a decrease in their mitotic and proliferative activity compared to the control, both in the cancer tissue itself and in the zone of its invasion into the adjacent muscle tissue. This leads to a significant decrease in cancer invasiveness, up to its complete block with prominent DR.

It was shown that the number of CSCs (according to ALDH1, CD34, CD133) in LLC is 20–30% of all cancer cells. The proportion of CSCs among surviving LLC cells decreases after PDT with $(3\text{-PyBrE})_4BCBr_4$ and $(3\text{-PyEPy})_4BCBr_8$ by 2.7–3.5 and 12.7–15.5 times, respectively. Taking into account the decrease in the number of surviving LLC cells, PDT with $(3\text{-PyBrE})_4BCBr_4$ inhibits the number of cancer stem cells by more than 20 times, and PDT with $(3\text{-PyEPy})_4BCBr_8$ by more than 100 times. It can be attributed to the charge-

dependent electrostatic binding of PS molecules to the surface of the lipid bilayer of a cancer cell, as well as to a more efficient charge-dependent penetration through this bilayer, as was suggested in [27].

It has been shown that vascularization in LLC mouse models occurs due to CSCs. These cells are capable of transforming into endothelium through the mechanism of epithelial-mesenchymal transformation and form tumor vessels. It suggests that the mechanism of LLC vascularization is based on the transformation of CD34+ CSCs and may be similar to stem cell vasculogenesis in embryonic tissues. Our results are consistent with those of other authors who have found vasculogenesis in malignant tumors—melanomas, breast and kidney carcinomas [28].

It has been established that PSs (3-PyBrE)$_4$BCBr$_4$ and (3-PyEPy)$_4$BCBr$_8$ exhibit high phototoxicity against LLC cells, but do not have a cytopathic effect on human endothelial cells (HUVEC) either in dark conditions or under irradiation [21]. The experiment showed high selective sensitivity to PDT with (3-PyBrE)$_4$BCBr$_4$ and (3-PyEPy)$_4$BCBr$_8$ only in the endothelium of newly formed LLC tumor vessels, while the vascular endothelium in intact tissues adjacent to the carcinoma remained intact. Our study found that a decrease in vascularization in LLC carcinoma tissue occurs along with the death of CSCs, since the source of new vessels in the cancer tumor disappears. An important aspect of the disruption of neoangiogenesis in a tumor during PDT with polycationic PSs is the destruction of CSC niches that support CSC viability.

PDT with polycationic derivatives of bacteriochlorin charge-dependently induces a pronounced desmoplastic reaction. This reaction is more pronounced in PDT with (3-PyEPy)$_4$BCBr$_8$ compared to PDT with (3-PyBrE)$_4$BCBr$_4$, and leads to the formation of granulation tissue at the tumor border.

5. Conclusions

It has been shown that polycationic PSs based on polycationic derivatives of synthetic bacteriochlorin destroy CSCs and tumor neovascularization, while also activating the desmoplastic reaction. This presents new opportunities for increasing the treatment effectiveness and reducing the occurrence of relapses and metastasis after PDT.

Author Contributions: Conceptualization, E.K., G.M., Z.C., V.L. (Victor Loschenov) and I.R. (Igor Reshetov); Data curation, E.K., G.M., I.M., N.Z. and S.D.; Formal analysis, E.A.; Funding acquisition, I.R. (Igor Reshetov); Investigation, E.K., G.M., S.K. (Saida Karshieva), E.M., I.R. (Igor Romanishkin) and E.A.; Methodology, E.K., G.M., S.K. (Saida Karshieva), I.M., N.Z., S.K. (Sergey Kharnas), V.L. (Vladimir Levkin) and S.D.; Project administration, I.R. (Igor Reshetov); Resources, V.L. (Victor Loschenov) and I.R. (Igor Reshetov); Supervision, Z.C., V.L. (Victor Loschenov) and I.R. (Igor Reshetov); Visualization, I.R. (Igor Romanishkin); Writing—original draft, E.K. and G.M.; Writing—review and editing, I.R. (Igor Romanishkin). All authors have read and agreed to the published version of the manuscript.

Funding: This work was funded by Russian Science Foundation and National Natural Science Foundation of China according to the bilateral Russian–Chinese project (RSF grant No. 24-45-00020, NSFC grant No. 22361132541).

Institutional Review Board Statement: The work with animals was carried out in compliance with international recommendations for conducting research using laboratory animals set forth in the "European Convention for the Protection of Vertebrate Animals used for Experimental and other Scientific Purposes" (Strasbourg, 1987). The study was approved by the local ethical committee at Sechenov University, Moscow, Russia (excerpt #25-22, 8 December 2022).

Informed Consent Statement: Not applicable.

Data Availability Statement: The data presented in this study are available upon request from the corresponding author.

Conflicts of Interest: The authors declare no conflicts of interest.

References

1. Averyanov, A. (Ed.) *Difficult to Diagnose Rare Diffuse Lung Disease*; Elsevier: Amsterdam, The Netherlands, 2020; ISBN 978-0-12-815375-8.
2. Goldblum, J.R.; Lamps, L.W.; McKenney, J.K.; Myers, J.L.; Ackerman, L.V.; Rosai, J. (Eds.) *Rosai and Ackerman's Surgical Pathology—2 Volume Set*, 11th ed.; Elsevier: Philadelphia, PA, USA, 2018; ISBN 978-0-323-26339-9.
3. Kumar, V.; Abbas, A.K.; Aster, J.C.; Turner, J.R.; Perkins, J.A.; Robbins, S.L.; Cotran, R.S. (Eds.) *Robbins & Cotran Pathologic Basis of Disease*, 10th ed.; Elsevier: Philadelphia, PA, USA, 2021; ISBN 978-0-323-53113-9.
4. Allison, R.R.; Moghissi, K. Photodynamic Therapy (PDT): PDT Mechanisms. *Clin. Endosc.* **2013**, *46*, 24. [CrossRef] [PubMed]
5. Prabavathy, D.; Swarnalatha, Y.; Ramadoss, N. Lung Cancer Stem Cells—Origin, Characteristics and Therapy. *Stem Cell Investig.* **2018**, *5*, 6. [CrossRef] [PubMed]
6. Caon, I.; Bartolini, B.; Parnigoni, A.; Caravà, E.; Moretto, P.; Viola, M.; Karousou, E.; Vigetti, D.; Passi, A. Revisiting the Hallmarks of Cancer: The Role of Hyaluronan. *Semin. Cancer Biol.* **2020**, *62*, 9–19. [CrossRef] [PubMed]
7. De Aberasturi, A.L.; Redrado, M.; Villalba, M.; Larzabal, L.; Pajares, M.J.; Garcia, J.; Evans, S.R.; Garcia-Ros, D.; Bodegas, M.E.; Lopez, L.; et al. TMPRSS4 Induces Cancer Stem Cell-like Properties in Lung Cancer Cells and Correlates with ALDH Expression in NSCLC Patients. *Cancer Lett.* **2016**, *370*, 165–176. [CrossRef] [PubMed]
8. Mohiuddin, I.S.; Wei, S.-J.; Kang, M.H. Role of OCT4 in Cancer Stem-like Cells and Chemotherapy Resistance. *Biochim. Biophys. Acta BBA—Mol. Basis Dis.* **2020**, *1866*, 165432. [CrossRef]
9. Lemjabbar-Alaoui, H.; Hassan, O.U.; Yang, Y.-W.; Buchanan, P. Lung Cancer: Biology and Treatment Options. *Biochim. Biophys. Acta BBA—Rev. Cancer* **2015**, *1856*, 189–210. [CrossRef] [PubMed]
10. Islam, F.; Gopalan, V.; Smith, R.A.; Lam, A.K.-Y. Translational Potential of Cancer Stem Cells: A Review of the Detection of Cancer Stem Cells and Their Roles in Cancer Recurrence and Cancer Treatment. *Exp. Cell Res.* **2015**, *335*, 135–147. [CrossRef] [PubMed]
11. Zhang, Z.-J.; Wang, K.-P.; Mo, J.-G.; Xiong, L.; Wen, Y. Photodynamic Therapy Regulates Fate of Cancer Stem Cells through Reactive Oxygen Species. *World J. Stem Cells* **2020**, *12*, 562–584. [CrossRef] [PubMed]
12. Morgan, J.; Jackson, J.D.; Zheng, X.; Pandey, S.K.; Pandey, R.K. Substrate Affinity of Photosensitizers Derived from Chlorophyll-a: The ABCG2 Transporter Affects the Phototoxic Response of Side Population Stem Cell-like Cancer Cells to Photodynamic Therapy. *Mol. Pharm.* **2010**, *7*, 1789–1804. [CrossRef]
13. Crous, A.; Dhilip Kumar, S.S.; Abrahamse, H. Effect of Dose Responses of Hydrophilic Aluminium (III) Phthalocyanine Chloride Tetrasulphonate Based Photosensitizer on Lung Cancer Cells. *J. Photochem. Photobiol. B Biol.* **2019**, *194*, 96–106. [CrossRef]
14. Chizenga, E.P.; Chandran, R.; Abrahamse, H. Photodynamic Therapy of Cervical Cancer by Eradication of Cervical Cancer Cells and Cervical Cancer Stem Cells. *Oncotarget* **2019**, *10*, 4380–4396. [CrossRef]
15. Aniogo, E.C.; Plackal Adimuriyil George, B.; Abrahamse, H. The Role of Photodynamic Therapy on Multidrug Resistant Breast Cancer. *Cancer Cell Int.* **2019**, *19*, 91. [CrossRef] [PubMed]
16. Tumangelova-Yuzeir, K.; Minkin, K.; Angelov, I.; Ivanova-Todorova, E.; Kurteva, E.; Vasilev, G.; Arabadjiev, J.; Karazapryanov, P.; Gabrovski, K.; Zaharieva, L.; et al. Alteration of Mesenchymal Stem Cells Isolated from Glioblastoma Multiforme under the Influence of Photodynamic Treatment. *Curr. Issues Mol. Biol.* **2023**, *45*, 2580–2596. [CrossRef]
17. Kogan, E.A.; Meerovich, G.A.; Karshieva, S.S.; Makarova, E.A.; Romanishkin, I.D.; Akhlyustina, E.V.; Meerovich, I.G.; Zharkov, N.V.; Demura, T.A.; Chen, Z.-L.; et al. On the Mechanisms of Photodynamic Action of Photosensitizers Based on Polycationic Derivatives of Synthetic Bacteriochlorin against Human Lung Cancer Cells A549 (in Vitro Study). *Photodiagnosis Photodyn. Ther.* **2022**, *39*, 102955. [CrossRef] [PubMed]
18. Koudinova, N.V.; Pinthus, J.H.; Brandis, A.; Brenner, O.; Bendel, P.; Ramon, J.; Eshhar, Z.; Scherz, A.; Salomon, Y. Photodynamic Therapy with Pd-bacteriopheophorbide (TOOKAD): Successful *in Vivo* Treatment of Human Prostatic Small Cell Carcinoma Xenografts. *Int. J. Cancer* **2003**, *104*, 782–789. [CrossRef]
19. Ethirajan, M.; Chen, Y.; Joshi, P.; Pandey, R.K. The Role of Porphyrin Chemistry in Tumor Imaging and Photodynamic Therapy. *Chem. Soc. Rev.* **2011**, *40*, 340–362. [CrossRef]
20. Yakubovskaya, R.I.; Plotnikova, E.A.; Plyutinskaya, A.D.; Morozova, N.B.; Chissov, V.I.; Makarova, E.A.; Dudkin, S.V.; Lukyanets, E.A.; Vorozhtsov, G.N. Photophysical Properties and in Vitro and in Vivo Photoinduced Antitumor Activity of Cationic Salts of Meso-Tetrakis(N-Alkyl-3-Pyridyl)Bacteriochlorins. *J. Photochem. Photobiol. B Biol.* **2014**, *130*, 109–114. [CrossRef]
21. Kogan, E.A.; Meerovich, G.A.; Karshieva, S.S.; Makarova, E.A.; Romanishkin, I.D.; Akhlyustina, E.V.; Meerovich, I.G.; Zharkov, N.V.; Koudan, E.V.; Demura, T.A.; et al. Photodynamic Therapy of Lung Cancer with Photosensitizers Based on Polycationic Derivatives of Synthetic Bacteriochlorin (Experimental Study). *Photodiagnosis Photodyn. Ther.* **2023**, *42*, 103647. [CrossRef]
22. Makarova, E.A.; Lukyanets, E.A.; Tiganova, I.G.; Romanova, Y.M.; Meerovich, G.A.; Loschenov, V.B.; Alekseeva, N.V.; Akhlyustina, E.V. Photosensitizers for Photodynamic Inactivation of Bacteria, Including in Biofilms. RU Patent #2670201, 13 June 2018. Available online: https://patents.google.com/patent/RU2670201C1/en (accessed on 8 April 2024).
23. Yakubovskaya, R.I.; Kazachkina, N.I.; Karmakova, T.A.; Morozova, N.B.; Pankratov, A.A.; Plyutinskaya, A.D.; Feofanov, A.V.; Chissov, V.I.; Tikhomirova, A.V. Methodological Recommendations for the Study of Photoinduced Antitumor Properties of Pharmaceuticals. In *Guidelines for Conducting Preclinical Studies of Pharmaceuticals*; Grif&K: Tula, Russia, 2012; Volume 1, pp. 655–669.
24. Kumar, G.L.; Rudbeck, L. (Eds.) *Immunohistochemical Staining Methods*, 5th ed.; DAKO Corporation: Glostrup, Denmark, 2009.
25. Wilcoxon, F. Individual Comparisons by Ranking Methods. *Biom. Bull.* **1945**, *1*, 80–83. [CrossRef]

26. Zheng, H.; Pomyen, Y.; Hernandez, M.O.; Li, C.; Livak, F.; Tang, W.; Dang, H.; Greten, T.F.; Davis, J.L.; Zhao, Y.; et al. Single-cell Analysis Reveals Cancer Stem Cell Heterogeneity in Hepatocellular Carcinoma. *Hepatology* **2018**, *68*, 127–140. [CrossRef]
27. Orekhov, P.S.; Kholina, E.G.; Bozdaganyan, M.E.; Nesterenko, A.M.; Kovalenko, I.B.; Strakhovskaya, M.G. Molecular Mechanism of Uptake of Cationic Photoantimicrobial Phthalocyanine across Bacterial Membranes Revealed by Molecular Dynamics Simulations. *J. Phys. Chem. B* **2018**, *122*, 3711–3722. [CrossRef]
28. Li, F.; Xu, J.; Liu, S. Cancer Stem Cells and Neovascularization. *Cells* **2021**, *10*, 1070. [CrossRef]